Supplementary Material (ESI) for Chemical Communication
This journal is (c) The Royal Society of Chemistry 2013

Electronic Supplementary Information

Nitric Oxide-generating L-cysteine-grafted Graphene Film as A Blood-contacting Biomaterial

Zhen Du,[a,b,†] Ruixia Dou,[a,b,†] Mian Zu,[b] Xueying Liu,[b] Wenyan Yin,[b] Yuliang Zhao,[b] Jingbo Chen,*[a] Liang Yan,*[b] and Zhanjun Gu*[b]

[a] *School of Materials Science & Engineering, Zhengzhou University, Zhengzhou 450002, China.*

[b] *CAS Key Laboratory for Biomedical Effects of Nanomaterials and Nanosafety, Institute of High Energy Physics, Chinese Academy of Sciences, Beijing 100049, China. Fax: +86-10-88236786.*

[†] *These authors contributed equally.*

E-mail: chenjb@zzu.edu.cn; yanliang@ihep.ac.cn, zjgu@ihep.ac.cn

1. Materials and Methods

Materials: Powder graphite (99%), chloroacetic acid ($ClCH_2COOH$， 98%), and sodium nitrite ($NaNO_2$, 97%) were purchased from Alfa Aesar. Branched-polyethylenimine (PEI, 25 kDa) and S-Nitroso-N-acetyl-DL-penicillamine (SNAP, ≥97%) were obtained from Sigma-Aldrich. L-cysteine (Cys, 98%) and N-ethyl-N'-[3-(dimethylamino)propyl]carbodiimide Hydrochloride (EDC, 99%) were supplied by J&K Chemical Ltd. Bovine serum albumin (BSA, Biological grade, >98%) was obtained from Amerso Company. Other reagents were purchased from Beijing Chemical Reagent Company. All the chemicals were of analytical grade and were used as received without further purification.

Synthesis of Graphene Oxide: Graphite oxide was synthesized from purified natural graphite via the Hummer's method with minor modification.[1, 2] Typically, natural graphite powder (1.0000 g) was mixed with concentrated H_2SO_4 (25 mL) and then $KMnO_4$ (3.5000 g) under vigorous stirring. Subsequently the mixture was heated to 37 °C and kept stirring for 2 h. 90 mL of deionized water and 25 mL of H_2O_2 solution (30%) were added to the above suspension to remove the residual manganese dioxide and potassium permanganate. On completion of the reaction, the mixture was washed with 5% hydrochloric acid and water, and sequentially was subjected to dialysis to remove residual metal ions and acid. Finally, graphene oxide (GO) nanosheets were prepared *via* bath-sonication of graphite oxide for 1 h, followed by centrifuging at 12 000 rpm for 10 min to remove unexfoliated graphite oxide.

Functionalization of graphene oxide: In order to attach PEI, we firstly converted -OH groups to -COOH groups using the method reported by Sun *et al.*[3] Briefly, 1.2000 g of NaOH and 1.0000 g of chloroacetic acid were added to GO suspension with the concentration of 1 mg/mL and then bath-sonicated for 3 h. Afterwards, the resultant suspension was neutralized by 5% hydrochloric acid, and then purified by repeated rinsing. The final production was carboxylic acid modified GO (GO-COOH).

In order to attach PEI, GO-COOH dispersion was diluted by deionized water until its concentration reached to ~1 mg/mL and was then bath-sonicated with PEI (10 mg/mL) for 10 min. EDC was then added to reach 5 mM and the resultant dispersion was bath-sonicated for another 30 min. Afterwards, more EDC was added to reach 20 mM and stirred for 24 h at room temperature. After centrifugation (42 000 rpm) of the resulting dispersion for 1 h, the precipitate was collected and washed several times with deionized water, and finally dispersed into water, obtaining the PEI functionalized GO (GO-COOH-PEI).

L-cysteine was further conjugated with GO-COOH-PEI by reaction between the -COOH groups on the L-cysteine molecules and free $-NH_2$ groups of the GO-COOH-PEI. Briefly, EDC was added to the mixture of GO-COOH-PEI and L-cysteine to reach 5 mM. After bath-sonication for 30 min, adequate EDC was added to the above mixture until the concentration of EDC reached up to 20 mM, and stirred overnight at room temperature. The unreacted species were separated out by centrifugation and subsequently dialysised against deionized water for 5 days with the water being changed twice per day. Finally, a stable black aqueous suspension of L-cysteine functionalized GO nanosheets could be obtained (GO-COOH-PEI-Cys).

Preparation of Functional Graphene Film: Graphene-based films were prepared by the vacuum filtration method. In brief, GO or GO-COOH-PEI-Cys dispersions were first diluted to ~1 mg/mL and then bath-sonicated.[4] Afterwards, the obtained dispersions were filtered through the microporous membrane (50-mm diameter, 0.22-μm pore size, Jiuding High-Tech) by vacuum filtration at room temperature. Followed by air-drying, GO and functional graphene films could be easily achieved after peeling off from the membrane. Notably, the thickness of the films could be adjusted *via* changing either the concentration of dispersion or the corresponding filtration volume.

Characterization: Fourier transform infrared (FT-IR) spectra were collected using the Fourier transform Bruker EQUINOX55 spectrometer with the KBr pellet technique. The micro-Raman spectroscopy (Reni-shaw inVia Raman Spectroscope) experiments were conducted under ambient conditions with 633-nm excitation from an argon ion

laser. Atomic force microscopy (AFM) analysis was performed on a scanning probe microscopy (SPM, Multimode 8, Bruke) under ambient conditions. Morphologies of graphene-based films and platelets were characterized using filed-emission scanning electron microscope (FE-SEM, S-4800, Hitachi, Japan) at an acceleration voltage of 10 kV. Ultraviolet-visible (UV-vis) absorption spectrophotometer (U-3900, Hitachi) was used for measurement of optical absorbance. Zeta potential analysis was conducted by using zeta potential analyzer (Brookhaven instruments, NanoBrook Omni, 280044). Mechanical measurements were taken with a dynamic mechanical analyser (DMA Q800, TA Instruments). The functional graphene film was cut into stripes with the size of 2×20 mm^2. The tensile modulus was calculated via fitting the stress-strain plots in the linear regime.

Measurement of the Amount of Nitric Oxide: Because the NO-releasing property of human albumin (AlbSNO) was similar with that of S-nitroso-bovine serum albumin (BSA-NO),[5] we chose BSA-NO instead of AlbSNO as the model NO donor for S-transnitrosation experiments. In this work, BSA-NO was synthesized according to a previously reported method.[6] Briefly, BSA (4 mmol) was added to ice-cold deionized water (20 mL), followed by dissolution upon addition of 0.5 M HCl. In order to initiate nitrosation of the thiol residue of BSA, excess sodium nitrite was added, causing the formation of nitrous acid, which served as the nitrosating agent. Subsequently, the reaction was kept in an ice-bath and stirred for 30 min. Finally, excess nitrite and HCl were removed by dialysis against deionized water under ice-bath for 4 h with the water being changed twice at intervals of 30 min. Finally, due to the unstable nature, the as-made BSA-NO solution was stored at -20 °C for not more than one week.

Due to its quick response time, detection limits (1 nM minimun.), and specificity toward NO, ISO-NOP sensor (World Precision Instruments, Inc.) was chose to detect the total amount of NO catalytic generation from BSA-NO. Prior to detection of NO amount, the sensor tip was immersed in the 15 ml of solution #1 (0.1 M H_2SO_4 and 0.1 M KI), allowing the probe to equilibrate with the solution under stirring. Then aliquots of solution #2 (50 μM $NaNO_2$) were added and the resulting data were used to construct a standard curve of the respective current versus concentration. After washing with deionized water several times, the electrode was immersed in the 14 ml of dispersions with different concentrations of GO, GO-COOH, GO-COOH-PEI or GO-COOH-PEI-Cys under stirring until it was equilibrated with PBS. Then BSA-NO solution was added to the above dispersion, and the current value began to be recorded for at least 1000 seconds from each sample. Finally, the obtained data were correlated with the standard curve, resulting in measurements of the total amount of NO. The amount of NO catalytic generation from SNAP was measured using the same protocol except changing BSA-NO to SNAP.

Measurement of Nitric Oxide Flux: NO generation from functional graphene film was aldo measured by ISO-NOP sensor. Specifically, functional graphene film was placed in the sample vial containing 14 mL of PBS. The probe was then immersed in PBS. After the probe was equilibrated with PBS under stirring, BSA-NO solution was added and simultaneously the current flux began to be recorded. The cumulative NO flux was calculated from the standard curve of the current versus concentration.

In Vitro **Hemolysis Assay:** Sprague Dawley rats (9-11 weeks old) were purchased from Vital River Laboratories (Beijing, China), and then were housed in polyproplene cages and were given free access to standard chow and water for the duration of the study. Fresh whole blood was obtained from the rats. All procedures were performed in compliance with the guidelines of institutional animal care and use committee (Institute of High Energy Physics, Beijing, China) and approved by the ethical committee of the CAS Key Laboratory for Biomedical Effects of Nanomaterials and Nanosafety (China). To assess the *in vitro* hemocompatibility of functional graphene film, 1 mL of blood sample was added to 2 mL of PBS containging ethylenediaminetetracetic acid (EDTA). After mixing, red blood cells (RBCs) were then separated from serum *via* centrifugation at 2000 rpm for 10 min. The precipitate was washed several times with PBS and finally diluted into 10 mL of PBS. Afterwards, 0.2 mL of diluted RBC suspension was taken out to mix with: i) 0.8 ml of PBS as a negative control, ii) 0.8 ml of deionized water as a positive control, and iii) 0.8 ml of PBS and functional graphene films with different sizes (1: 2×2 mm^2, 2: 5×5 mm^2 and 3: 10×10 mm^2).

All the mixtures were vortexed and kept at room temperature for 3 h and centrifuged at 12000 rpm for 5 min. The absorbance of supernatants at 541 nm was measured by UV-vis spectrograph. The hemolysis percent of RBCs was calculated using the following equation:

$$\text{Hemolysis prcent (\%)} = (A_{sample}\text{-}A_{negative})/(A_{positive}\text{-}A_{negative}) \times 100\%$$

where, A_{sample}, $A_{negative}$ and $A_{positive}$ are the absorbance of samples, the negative control and positive control, respectively.

Preparation of Platelet Suspension: Fresh whole blood (~5 mL) was drawn from a healthy female rats. The blood was collected in tube containing sodium citrate (3.8%, w/v) at 9:1 (v/v) ratio of blood to sodium citrate solution. The separation of platelet rich plasma (PRP) from red blood cells was achieved by centrifugation at 1 500 rpm for 15 min. Afterwards, half of the PRP was collested for further use and the other PRP was transferred to another tube and centrifuged at 3 000 g for 10 min to obtain the platelet pellet. Finally, the platelet pellet was then gently resuspended in HEPES-buffered Tyrode's solution for further use.

In Vitro Platelet Adhesion Studies: Platelet suspension with and without PPP was used to evaluate the effects of plasma constituents on platelet adhesion in the presence of L-cysteine functionalized functional film. The functional graphene film was cut into quadrate pieces (10×10 mm^2) and put into 6 well plates using GO film as controls (n=3). Then platelet suspension with and without PPP was added to the well plates, respectively, and incubated at 37 °C for 30 min. After incubation, the films were washed three times with Tyrode's buffer, and were treated by 2.5% glutaraldehyde for 4 h. For SEM analysis, all of samples were subsequently dehydrated by a series of gradient ethanol solutions (40, 50, 75, 80, 85, 90, 95, and 100%), followed with drying by critical point dryer

Human Umbilical Vein Endothelial Cells Adhesion In Vitro: Human Umbilical Vein Endothelial Cells (HUVECs) were cultured in Dulbecco's modified Eagles media (DMEM) with 10% Fetal Bovine Serum (FBS, Gibco, Gland Island, NY, USA), but without antibiotics, in a humidified atmosphere of 5% CO_2 at 37 °C, and media was changed in every day.

The cytotoxicity of functional graphene film was determined by Live/Dead viability/cytotoxicity Kit (Molecular Probes) on HUVECs. All of the samples were placed in fresh multi-well culture plate in duplicates, respectively. Then, cells were placed in the plate at a cell density of 2×10^3/well for HUVECs and were incubated at 37 °C for 48 h. After that, cells were stained with calcein acetoxymethyl ester (showing green fluorescence on live cells by binding with calcium) and ethidium homodimer (showing red fluorescence on dead cells by intercalating between the strands of DNA and RNA), then washed three times with PBS and visualized by fluorescence microscopy (Olympus IX71). The number of live cells was counted at six independent sites of each sample.

For cell proliferation study, GO and functional graphene films were cut into quadrate pieces (10×10 mm^2) and put into 6 well plates. HUVECs were then seeded at a density of 1×10^4 cells per well. Cell proliferation was tested on hours 12, 24, 48 using calcein acetoxymethyl ester.

For cell adhesion study, functional graphene films were cut into quadrate pieces (10×10 mm^2) and put into 6 well plates, using GO film and tissue culture polystyrene film as control. Into each well was added 1×10^4 of HUVECs. After incubation for 24 h, samples were fixed in 4% paraformaldehyde, stained with Actin-Trakcer Green (50 μL per sample, lucifuge for 1 h), and visualized by fluorescence microscopy (Olympus IX71).

Statistical Analysis: All experiments were performed at least three independent times and data were reported as means ± standard deviation (SD) except as noted. Statistical significance between was determined using a T-test where a value of $p<0.05$ was considered to be significant and $p<0.01$ very significant.

2. Supplementary Data and Further Discussion

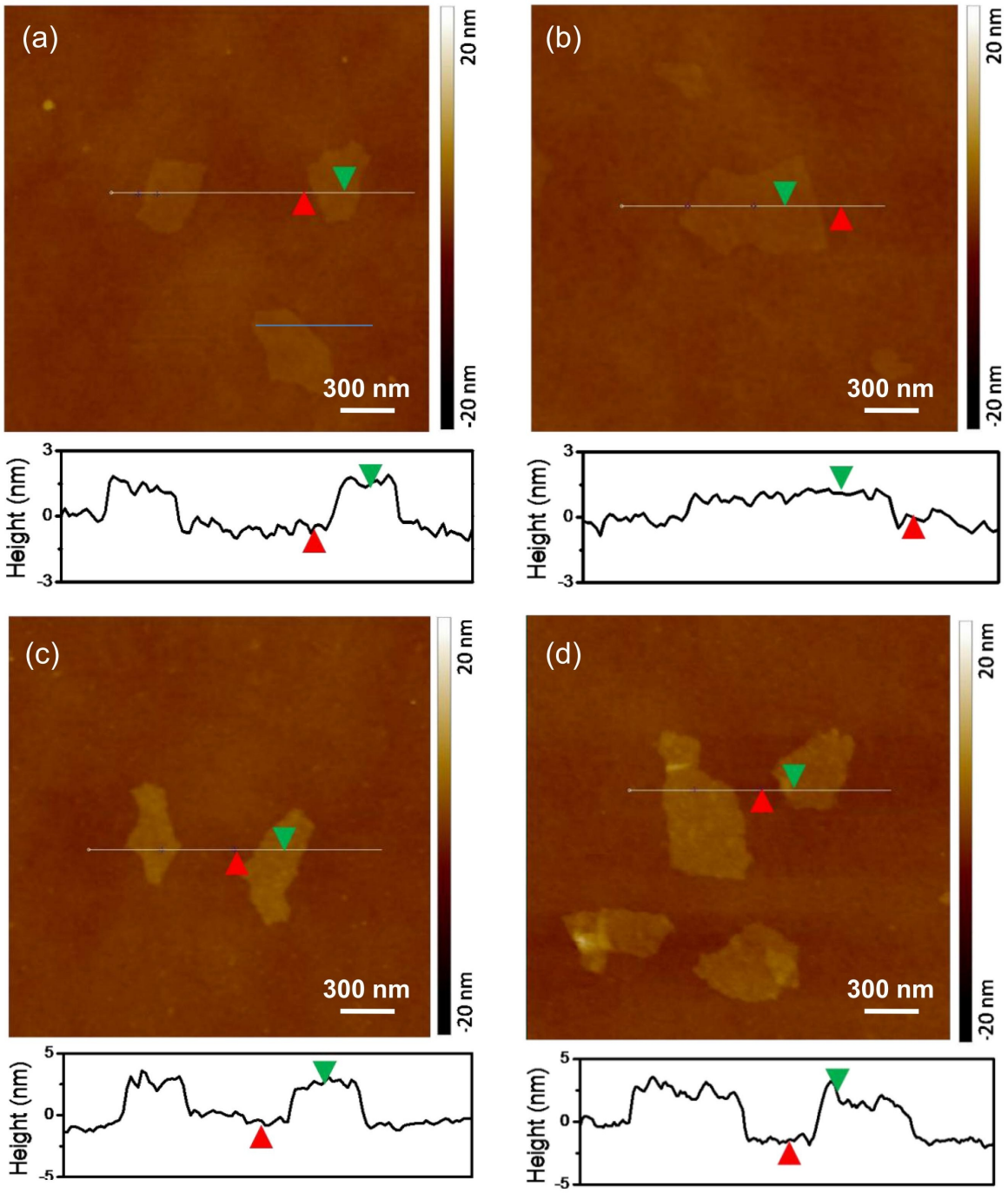

Fig. S1 AFM images of GO, (a) GO-COOH, (b) GO-COOH-PEI (c) and GO-COOH-PEI-Cys (d). According to AFM analysis, the thickness of GO nanosheets was ~1.2 nm, indicating that most of them were single layer GO. After activation with $ClCH_2COOH$ under strong basic conditions, there was no significant change of the thickness. However, after mixing with PEI solution, the thickness of GO nanosheets increased to 4-5 nm, indicating that PEI molecules were covalently attached on the surface of GO-COOH through the formation of an amide bond by the reaction between -COOH groups of GO-COOH and $-NH_2$ groups of PEI. Moreover, after successful conjugation of L-cysteine to GO-COOH-PEI through EDC chemistry, it was found that the thickness of nanosheets was further increased to 6-8 nm.

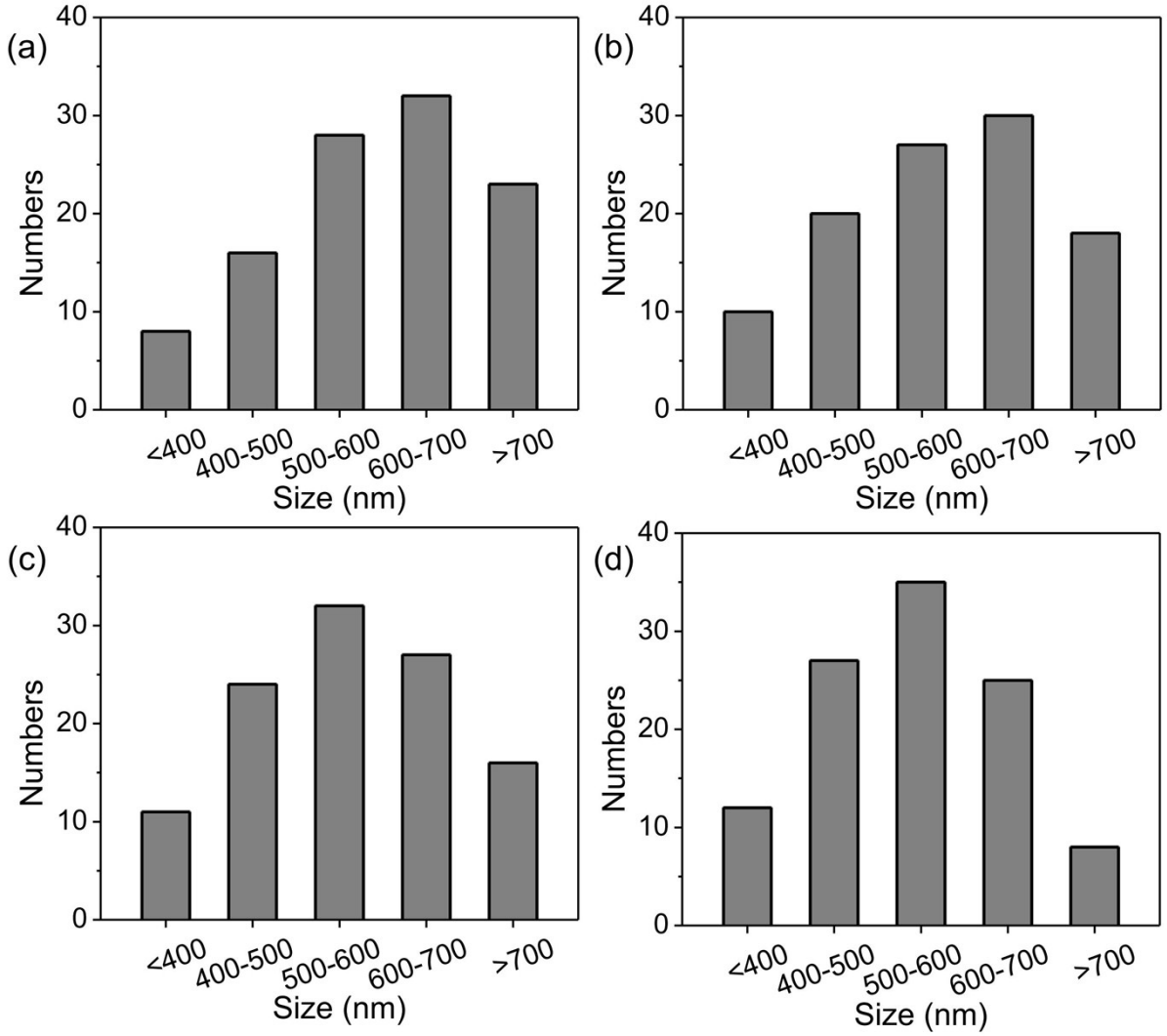

Fig. S2 Size distributions of GO (a), GO-COOH (b), GO-COOH-PEI (c) and GO-COOH-PEI-Cys (d). It was found that the size of GO nanosheets becomes smaller after functionalization.

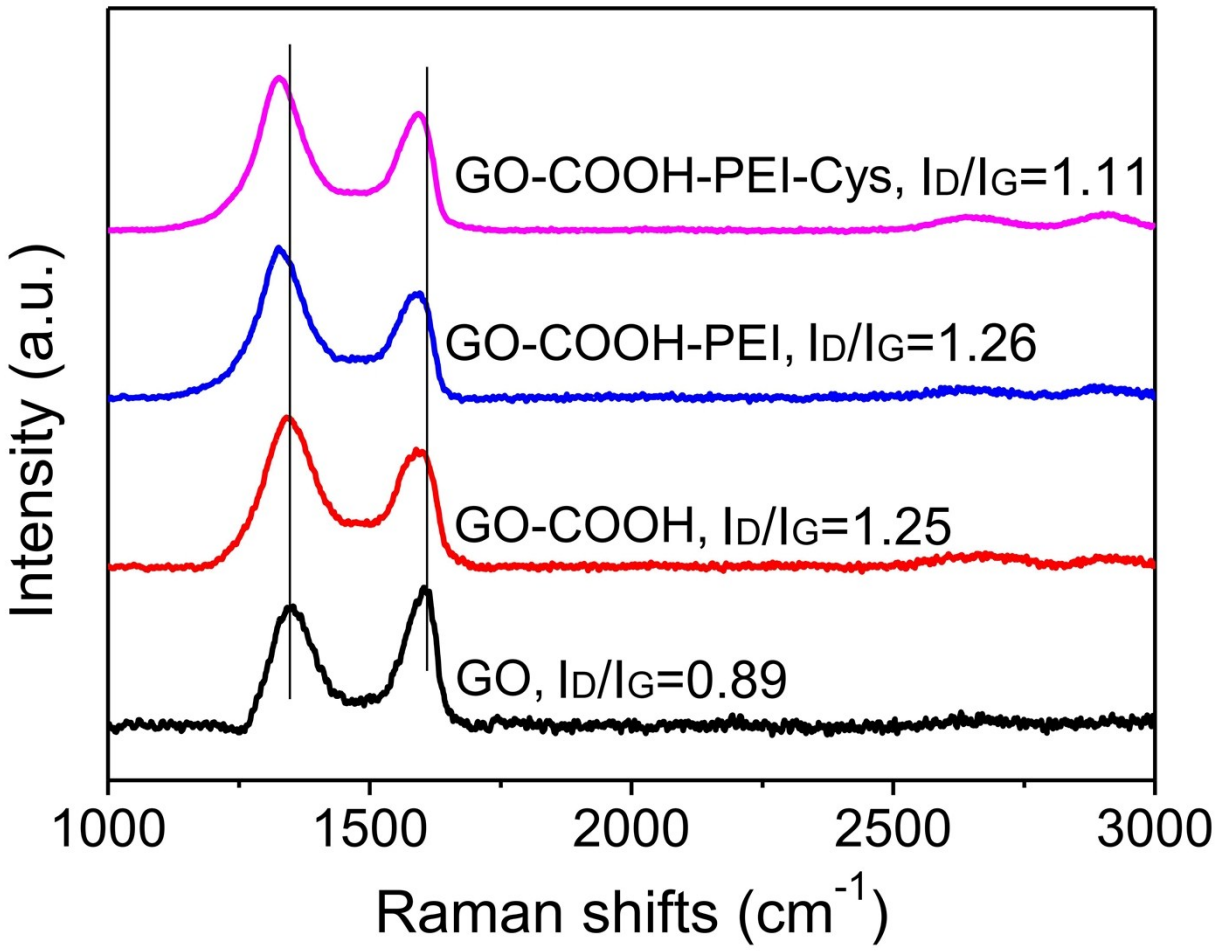

Fig. S3 Raman spectra of GO, GO-COOH, GO-COOH-PEI and GO-COOH-PEI-Cys. For GO nanosheets, it was well recognized that D band (~1346 cm^{-1}) arises from a breathing mode of κ-point photons of A_{1g} symmetry, while the G band (~1608 cm^{-1}) results from the first order scattering of the E_{2g} photon of sp^2 carbon atoms.[7] After activation, the G band of GO-COOH blue-shifted to 1595 cm^{-1} due to the influence of defects and isolated double bonds; while there was no significant change on the D band. In addition to the incrase of I_D/I_G ratio from 0.89 to 1.25, it indicates that more defects are formed during the activation process. When functionalization with PEI, both D band and G band decreased to 1325 and 1590 cm^{-1}, respectively, which were 21 and 5 cm^{-1} lower than those of GO-COOH. The blue-shift of D bands may be due to the molecular charge transfer between GO and PEI and the blue-shift of G bands arose from both the change transfer and the influence of defects and isolated double bonds. These results clearly afford support for the covalent attachment of PEI to GO via EDC chemistry. Moreover, conjugation of L-cysteine to GO-COOH-PEI resulted in the further decrease to 1322 cm^{-1}.

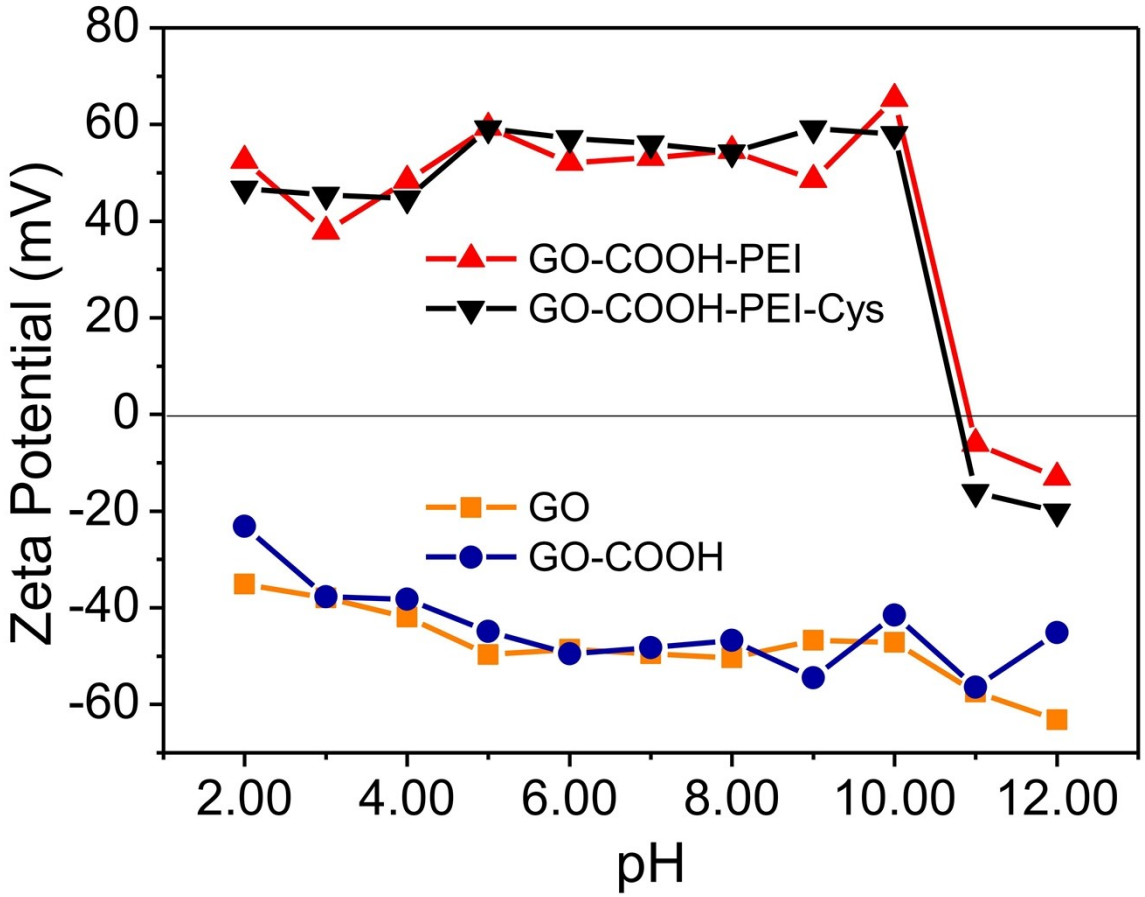

Fig. S4 Zeta potential of GO, GO-COOH, GO-COOH-PEI and GO-COOH-PEI-Cys in water with different pH values. it was found that the surface of GO and GO-COOh was negatively charged (zeta potential = −35−63 mV for GO and −24−46 mV for GO-COOH) over the investigated pH range (2.00-12.00), indicating the presence of plentiful –COOH groups.[8] However, after chemical functionalization with PEI and further with L-cysteine, the zeta potential of GO-COOH-PEI and GO-COOH-PEI-Cys significantly changed from negative to positive, consistent with the presence of free -NH_2 groups at the surface of graphene. Significantly, the free amino groups at the surface of GO-COOH-PEI served as the reactive activity sites facilitated subsequently chemical binding of as more as L-cysteine molecules to graphene.[4]

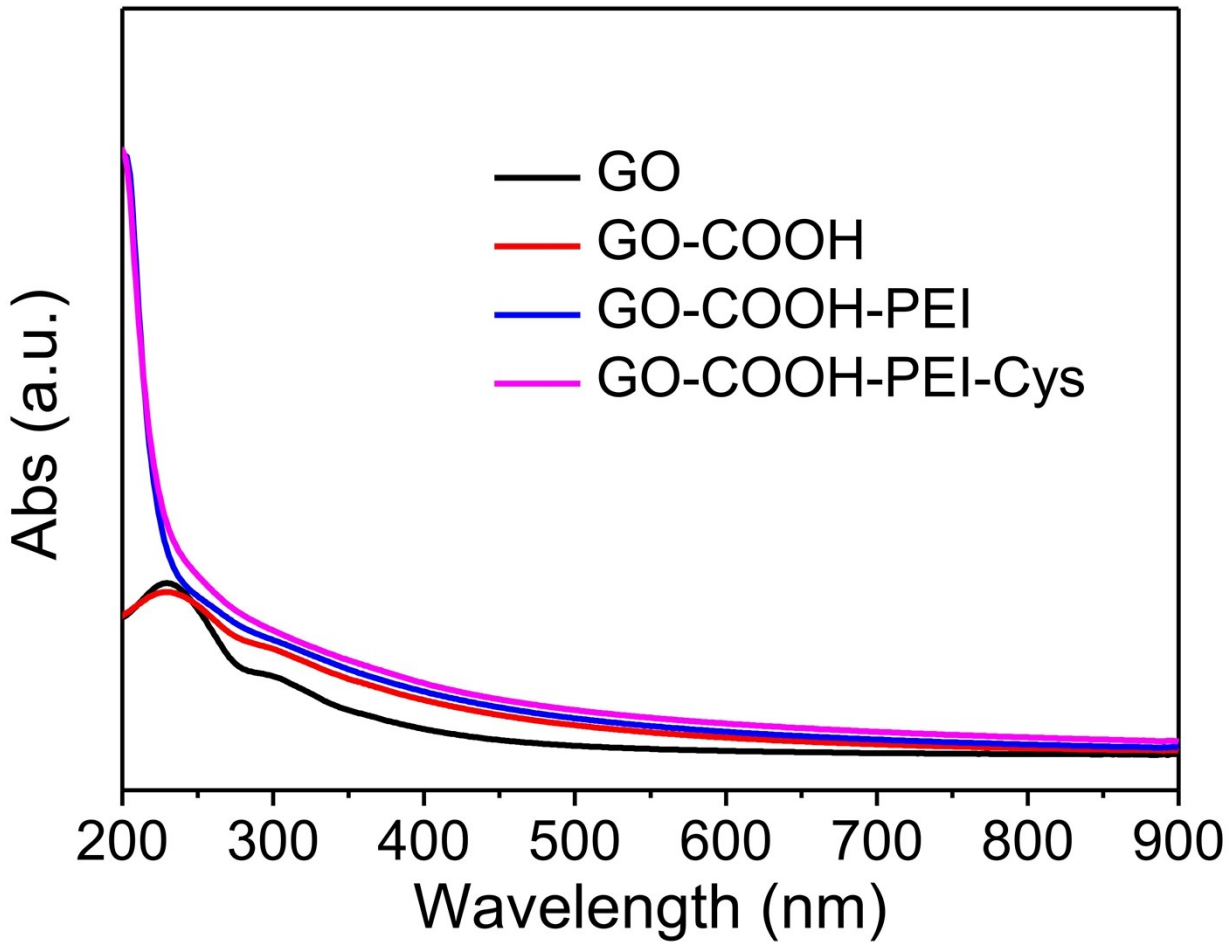

Fig. S5 UV-vis spectra of GO, GO-COOH, GO-COOH-PEI and GO-COOH-PEI-Cys. After PEI and further L-cysteine functionalization, a peak at 230 nm disappeared while a new peak at 258 nm appeared mainly due to the presence of PEI and L-cysteine in the grpahene.[9]

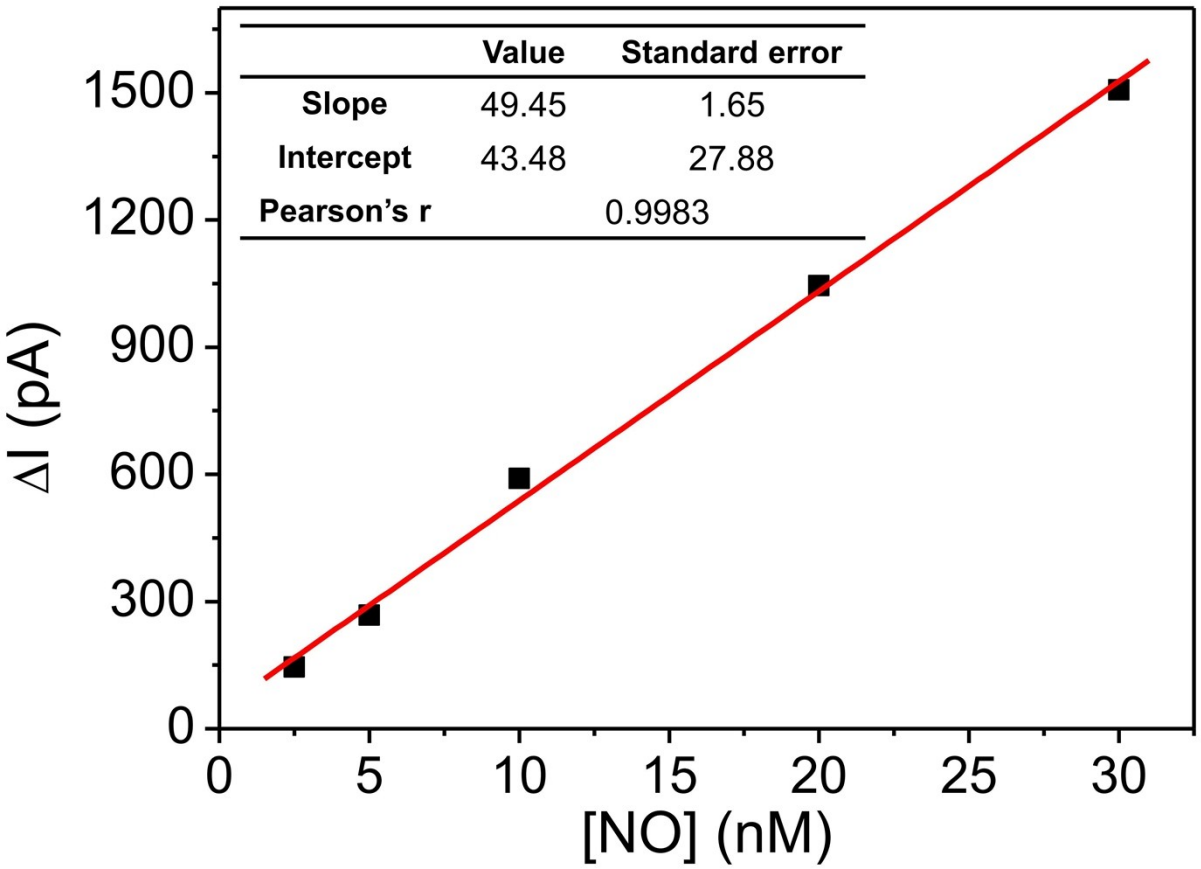

Fig. S6 The standard curve of the respective current versus concentration, which was applied to calculate the total amount of NO catalytic generation from NO donors.

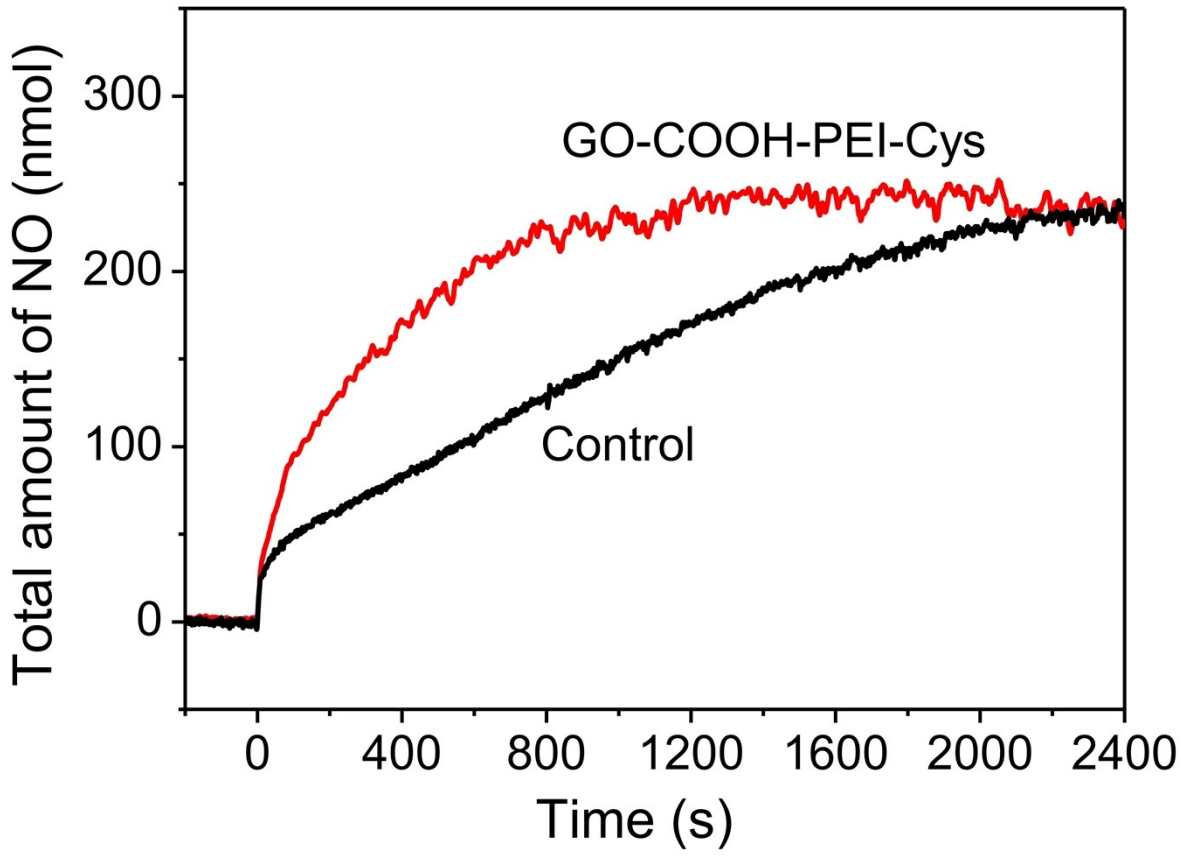

Fig. S7 The total amount of NO generation from SNAP after adding GO-COOH-PEI-Cys. This indicates that the immobilized L-cysteine, like free L-cysteine, was capable of extracting NO from SNAP to GO-COOH-PEI-Cys and then releasing NO from GO-COOH-PEI-Cys.

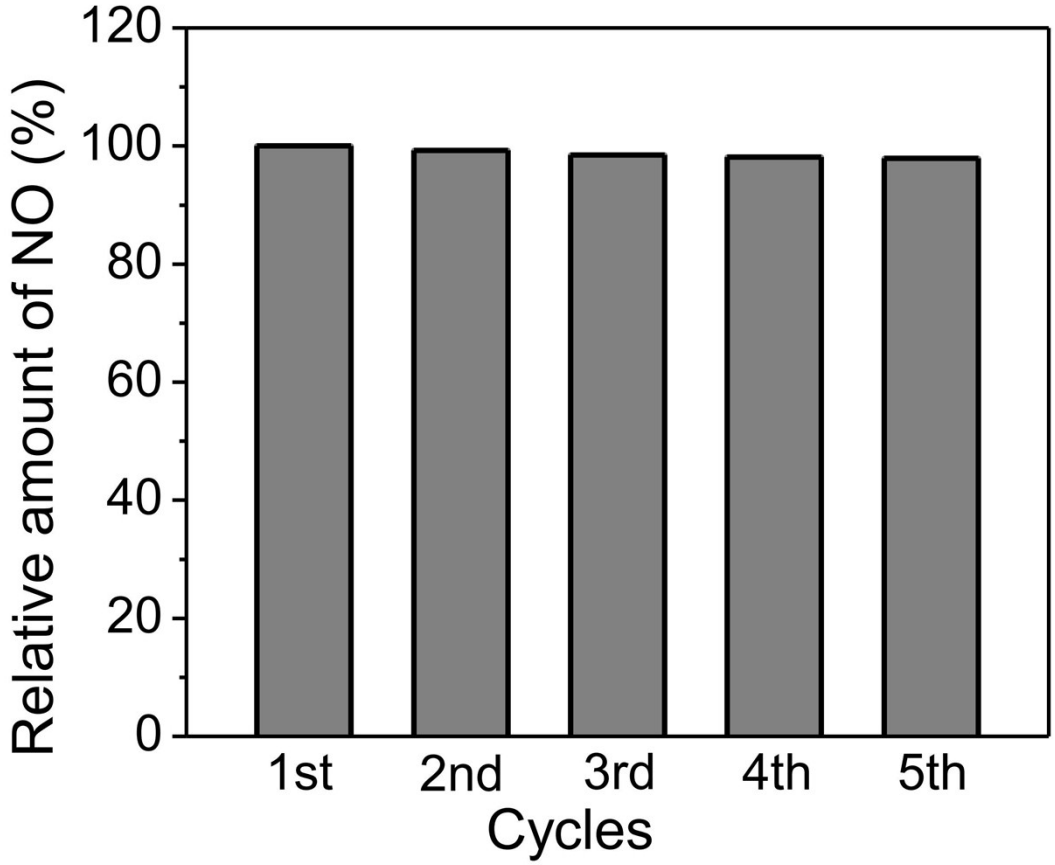

Fig. S8 Cycling runs in the decomposition of BSA-NO. The results showed the amount of NO decreased less than 5% after running five cycles, indicating good stability for decomposition of BSA-NO when exposed to physiological solution.

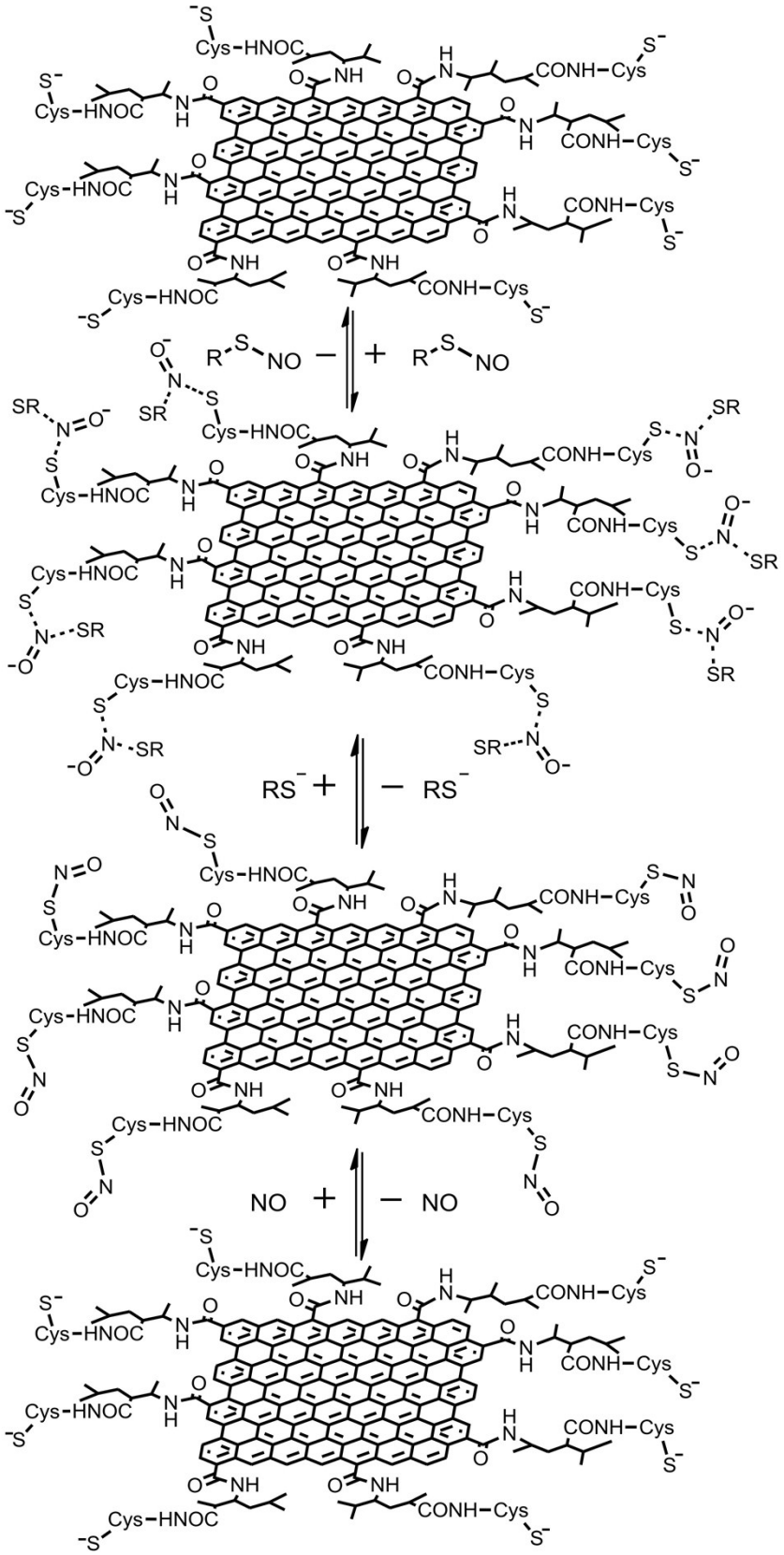

Fig. S9 Process of catalytic generation of NO from NO donors. First, nitroxyl disulfide intermediate (that is, [GO-COOH-PEI-Cys-SNOSR]$^{-}$) was obtained through transnitrosation reactions between RSNO and thiolate anions of the immobilizing L-cysteine of GO-COOH-PEI-Cys.[10] Due to the unstable nature, this intermediate then decomposed to get GO-COOH-PEI-Cys-SNO. Because Cys-NO, as a nitrosothiol, was less unstable than other nitrosothiols,[11, 12] GO-COOH-PEI-Cys-SNO could tend to further decompose to release NO.

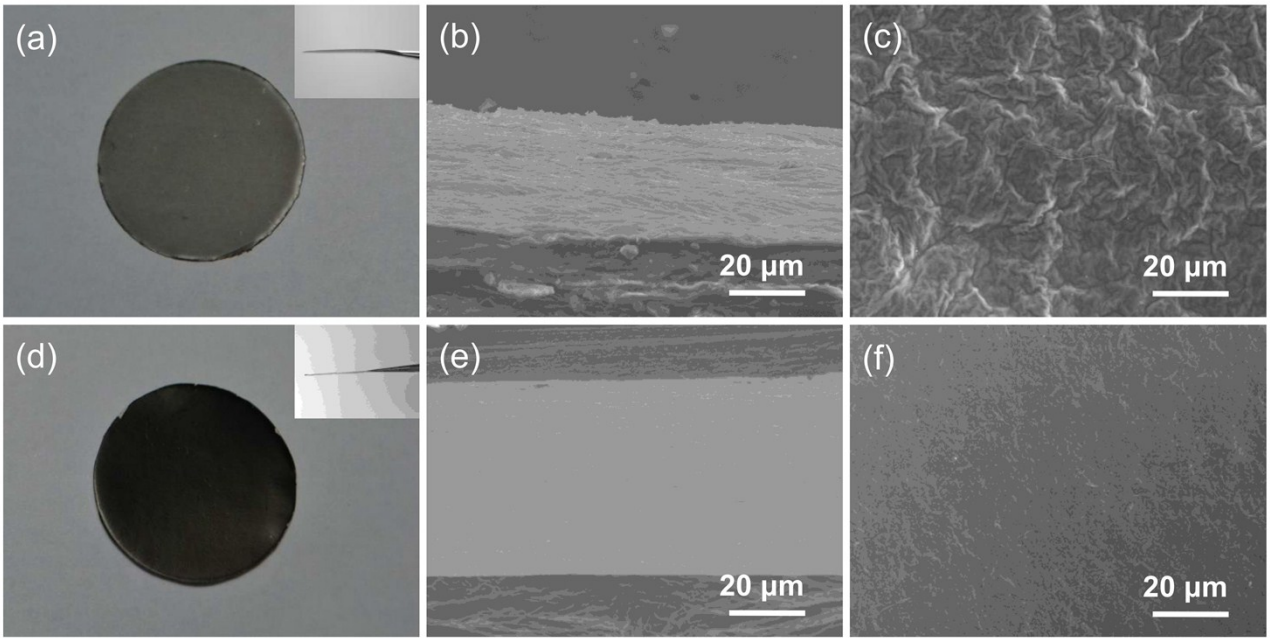

Fig. S10 (a) Photographs of GO film. **(b)** SEM side-view images of GO film. **(c)** Surface SEM image of GO film. **(d)** Photographs of functional graphene film. **(e)** SEM side-view images of functional graphene film. **(f)** Surface SEM image of functional graphene film.

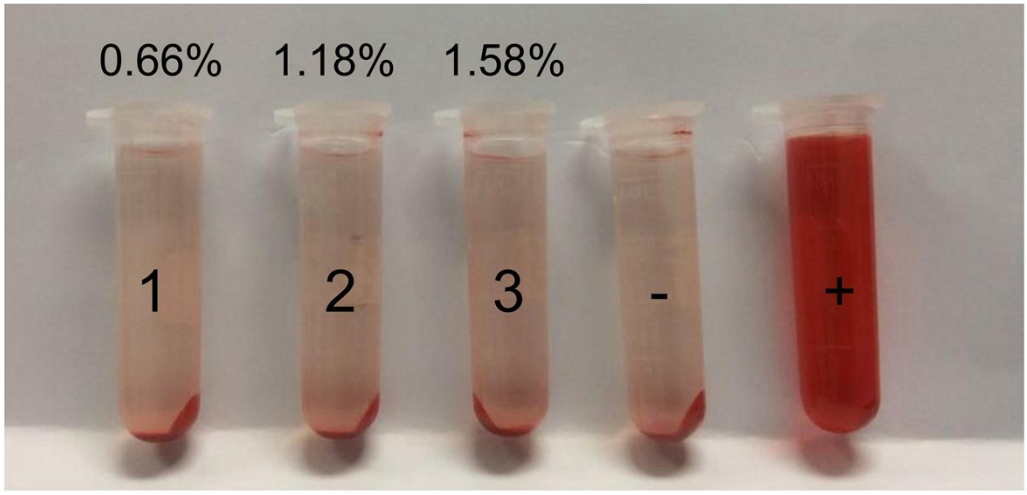

Fig. 11 The hemolytic percent of RBCs incubated with functional graphene films with different sizes (1: 2×2 mm^2, 2: 5×5 mm^2 and 3: 10×10 mm^2) for 3 h, using deionized PBS (–) and water (+) as negative and positive controls, respectively. This result suggests that functional graphene film exhibits good hemocompatibility.

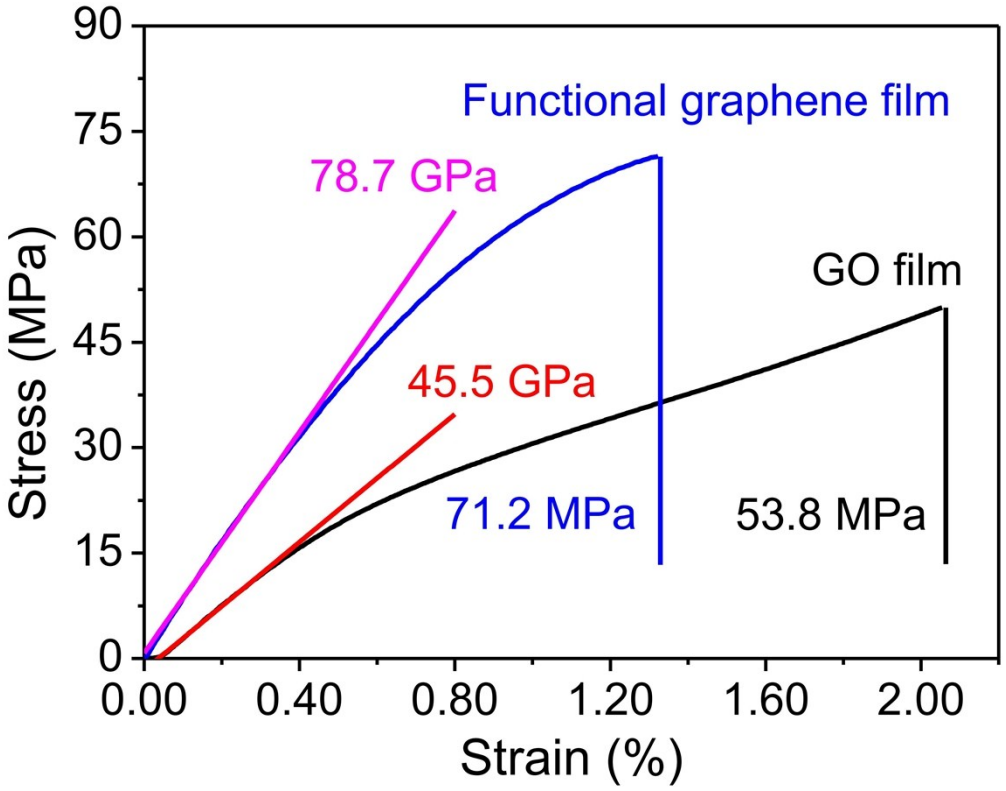

Fig. S12 Strain-stress plots of GO and functional graphene films.

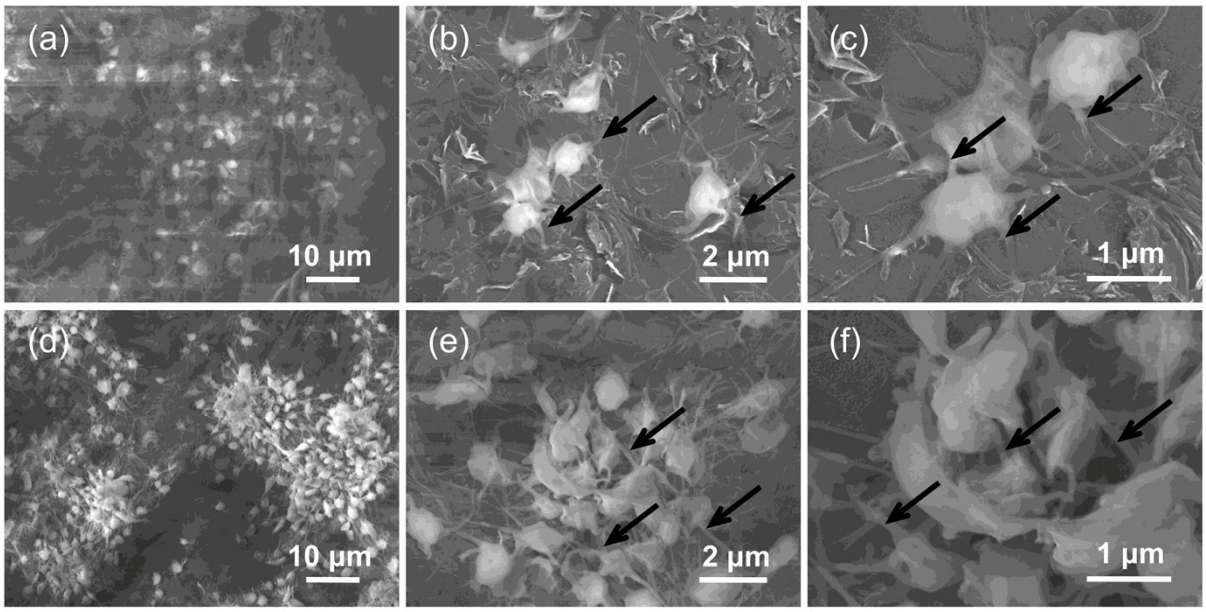

Fig. S13 Morphology of adhered platelets on GO films with (a-c) and without (d-f) addition of plasma.

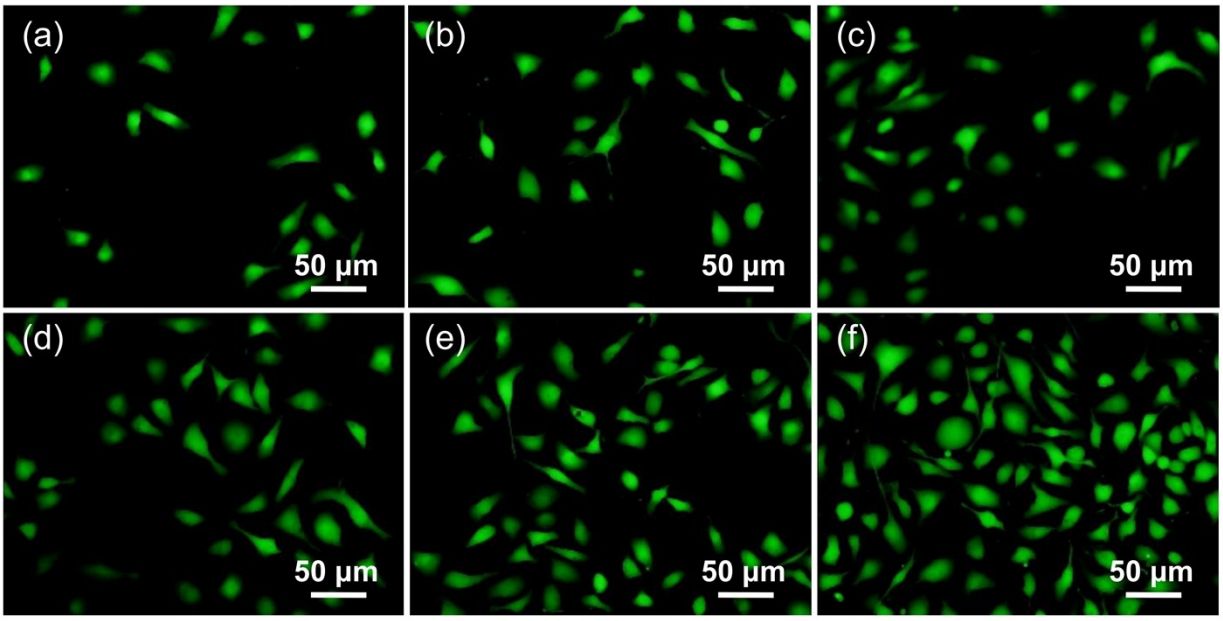

Fig. S14 Fluorescence staining of HUASMCs grown on the GO (a-c) and functional graphene (d-f) films after 12, 24 and 36 h of culture (From left to right).

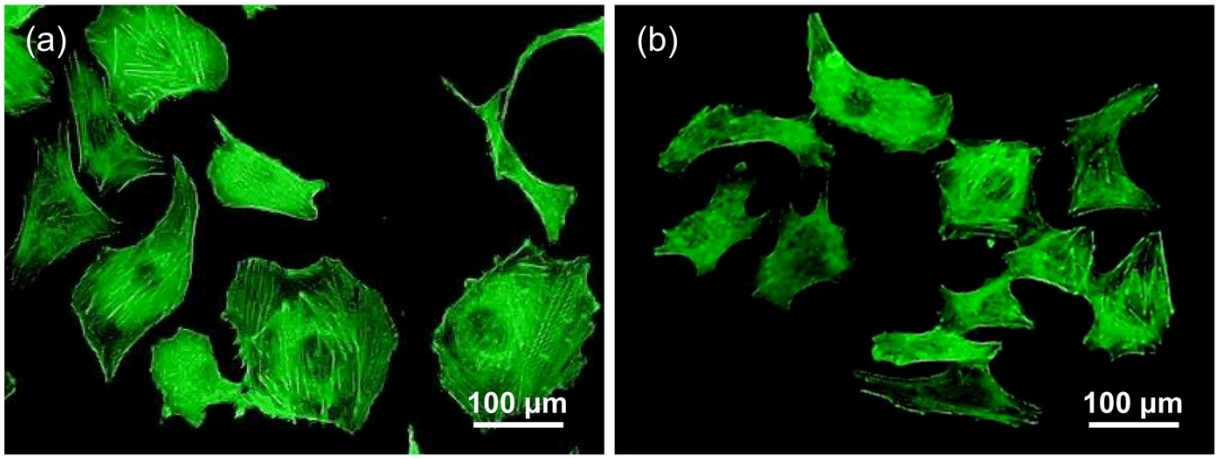

Fig. S15 Cell staining of HUVECs cultured on tissue culture polystyrene (a) and GO (b) films when cultured for 24 h.

1. L. Yan, Y.-N. Chang, L. Zhao, Z. Gu, X. Liu, G. Tian, L. Zhou, W. Ren, S. Jin, W. Yin, H. Chang, G. Xing, X. Gao and Y. Zhao, *Carbon*, 2013, **57**, 120.
2. L. Yan, Y.-N. Chang, W. Yin, X. Liu, D. Xiao, G. Xing, L. Zhao, Z. Gu and Y. Zhao, *Phys. Chem. Chem. Phys.,* 2014, **16**, 1576.
3. X. Sun, Z. Liu, K. Welsher, J. Robinson, A. Goodwin, S. Zaric and H. Dai, *Nano Res.,*2008, **1**, 203.
4. L. Yan, Y.-N. Chang, W. Yin, G. Tian, L. Zhou, Z. Hu, G. Xing, Z. Gu and Y. Zhao, *Adv. Eng. Mater.*, 2015, **17**, 523.
5. G. Scorza, D. Pietraforte and M. Minetti, *Free Radical Bio. Med.,* 1997, **22**, 633.
6. J. S. Stamler, O. Jaraki, J. Osborne, D. I. Simon, J. Keaney, J. Vita, D. Singel, C. R. Valeri and J. Loscalzo, *Proc. Natl. Acad. Sci. USA,* 1992, **89**, 7674.
7. E.-Y. Choi, T. H. Han, J. Hong, J. E. Kim, S. H. Lee, H. W. Kim and S. O. Kim, *J. Mater. Chem.,*2010, **20**, 1907.
8. S. Park and R. S. Ruoff, *Nat. Nanotechnol.*., 2009, **4**, 217.
9. L. Zhang, J. Xia, Q. Zhao, L. Liu and Z. Zhang, *Small*, 2010, **6**, 537
10. M. M. Melzer, E. Li and T. H. Warren, *Chem. Commun.,* 2009 , **39**,5847.
11. A. P. Dicks and D. L. H. Williams, *Chem. Biol.,* 1996, **3**, 655.
12. P. R. Myers, R. L. Minor, R. Guerra, J. N. Bates and D. G. Harrison, *Nature*, 1990, **345**, 161.